Scattering properties of an open quantum system

Agapi Emmanouilidou and L. E. Reichl
Center for Studies in Statistical Mechanics and Complex Systems, The University of Texas at Austin, Austin, Texas 78212
(Received 15 November 1999; published 18 July 2000)

We study the scattering properties of an open quantum system, in terms of the complex poles of the analytically continued energy Green's function. We use a model for which many dynamical properties can be expressed analytically. We first study particle wave scattering and compute the Wigner delay times. Then, using perturbation theory, we compute the photodetachment rate due to a weak time-periodic electric field. In addition, we show that the model we use qualitatively reproduces several features of the experimentally obtained photodetachment cross section of H^- ions and gives interesting insight into the mechanism underlying the photodetachment of H^- ions.

PACS number(s): 31.70.Hq, 03.65.Ge, 32.80.Gc, 34.50.−s

I. INTRODUCTION

The mechanisms underlying decay processes in open quantum systems are of great interest because they play a key role in the dynamics of mesoscopic and atomic systems. In order to elucidate some of these mechanisms we focus on a model consisting of single particle states in the presence of a δ-potential well and a static electric field. Ludviksson [1] showed that many of the dynamical properties of this model can be obtained analytically.

In this paper we study the scattering properties of this metastable system using generalized eigenstates associated with complex eigenvalues that are found by analytic continuation of the energy Green's function. In Sec. II, we review essential features of Ludviksson's description of the metastable system. In addition, we review the complex spectral decomposition of the survival probability, that was developed by Nickel and Reichl [2], for a certain class of initial states and is used in this paper to study light scattering. In Sec. III, we study particle wave scattering from the δ-potential well in the presence of a constant electric field. By determining the Wigner delay times we show the physical effect of the quasibound states associated with poles of the energy Green's function in the complex energy plane.

In Sec. IV, we study light scattering. We compute the photodetachment rate using the complex spectral decomposition mentioned above and directly interpret its main features in terms of the quasibound states. We find that the photodetachment rate oscillates as a function of photon energies. Similar oscillations have been observed experimentally in the photodetachment cross section of H^- ions [3–5] in the presence of static electric fields when using π polarized light. These oscillations have been predicted by a number of authors [6–10] who used three-dimensional theoretical models. However, these models do not account for the final state interaction of the detached electron with the neutral atom, as our model does. In Sec. IV, we discuss new effects that can occur when the final state interaction is included. We also offer a qualitative comparison with the experimental results which, we believe, gives interesting insight into the mechanism underlying the photodetachment of H^- ions.

In the Appendix, we briefly discuss some of the main features of the complex coordinate method [11,12] by applying the complex coordinate translation to our model. In Sec. V, we finish with some concluding remarks.

II. THE MODEL

The model we consider describes the behavior of a single particle, of mass m and charge q, in one space dimension, in the presence of a static electric field and a δ-function potential well. The one-dimensional Hamiltonian is

$$H(x)=-\frac{\hbar^2}{2m}\frac{\partial^2}{\partial x^2}-Fx-V'\delta(x), \tag{1}$$

where $\hbar$ is Planck's constant, F/q is the strength of the static electric field and V' is the strength of the δ-potential well. The above Hamiltonian has a continuum of energy eigenvalues over the interval $-\infty<E'<\infty$. If we introduce the dimensionless variables

$$\xi=x/x_0, \quad E=E'/\epsilon_0, \quad t=t'\epsilon_0/\hbar,$$

$$V=V'/x_0\epsilon_0, \quad z=z'/\epsilon_0, \quad \omega=\omega'\frac{\hbar}{\epsilon_0}, \tag{2}$$

where

$$x_0=\left(\frac{\hbar^2}{2mF}\right)^{1/3}, \quad \epsilon_0=Fx_0 \tag{3}$$

the Hamiltonian is given by

$$H(\xi)=-\frac{\partial^2}{\partial\xi^2}-\xi-V\delta(\xi). \tag{4}$$

Solving the Schrödinger equation

$$H(\xi)\Psi_E(\xi)=\left(-\frac{\partial^2}{\partial\xi^2}-\xi-V\delta(\xi)\right)\Psi_E(\xi)=E\Psi_E(\xi), \tag{5}$$

we find that the continuum energy eigenfunctions, $\Psi_E(\xi)=\langle\xi|E\rangle$, in Hilbert space, are given by

$$\Psi_E(\xi)=\begin{cases} N\mathrm{Ai}(-\xi-E), & \xi\leqslant 0, \\ N\{\mathrm{Ai}(-\xi-E)[1-V\pi\mathrm{Bi}(-E)\mathrm{Ai}(-E)]+\mathrm{Bi}(-\xi-E)V\pi\mathrm{Ai}^2(-E)\}, & \xi\geqslant 0, \end{cases} \tag{6}$$

where Ai and Bi are Airy functions [13] and

$$N=\frac{1}{\sqrt{[1-V\pi\mathrm{Bi}(-E)\mathrm{Ai}(-E)]^2+V^2\pi^2\mathrm{Ai}^4(-E)}}. \tag{7}$$

In the rest of this paper, we use dimensionless variables.

The retarded and advanced energy Green's functions of the system are given by $G^R(\xi,\xi',E+i\delta)=\langle\xi|(E-H+i\delta)^{-1}|\xi'\rangle$ and $G^A(\xi,\xi',E-i\delta)=\langle\xi|(E-H-i\delta)^{-1}|\xi'\rangle$, respectively, where δ is real and $\delta>0$. Ludviksson found that

$$G^{R/A}(\xi,\xi';z)=G_0^{R/A}(\xi,\xi';z)-\frac{G_0^{R/A}(\xi,0;z)G_0^{R/A}(0,\xi';z)}{1/V+G_0^{R/A}(0,0;z)}, \tag{8}$$

where $z=E+i\delta$ for the retarded energy Green's functions, G^R and G_0^R, and $z=E-i\delta$ for the advanced energy Green's functions, G^A and G_0^A. $G_0^{R/A}(\xi,\xi';z)$ are the retarded and advanced energy Green's functions when $V=0$, and are given by

$$G_0^{R/A}(\xi,\xi';z)=-\pi\times\begin{cases} \mathrm{Ai}(-\xi-z)\mathrm{Ci}^{\pm}(-\xi'-z), & \xi\leqslant\xi', \\ \mathrm{Ci}^{\pm}(-\xi-z)\mathrm{Ai}(-\xi'-z), & \xi\geqslant\xi', \end{cases} \tag{9}$$

where $\mathrm{Ci}^{\pm}=\mathrm{Bi}\pm i\,\mathrm{Ai}$.

The energy Green's functions, defined in Eqs. (8) and (9), are bounded when $\xi,\xi'\to\pm\infty$. The energy spectrum of the system described by the Hamiltonian H is determined by the singularities of the energy Green's functions. The Green's functions given by Eqs. (8) and (9), have a cut along the entire real energy axis and do not have any other singularities on the real axis. Due to causality, $G^{R/A}(\xi,\xi';z)$ for z on the upper/lower half energy plane have no singularities. If we analytically continue $G^R(\xi,\xi';z)$ on the lower half energy plane then $G^R(\xi,\xi';z)$ is no longer bounded when $\xi,\xi'\to\pm\infty$ and it has simple poles at complex values $z=z_n$. These simple poles are determined by the condition

$$\frac{1}{V}+G_0^R(0,0;z_n)=0, \tag{10}$$

and for every value of V, there is an infinite number of complex poles z_n. Similarly, if we analytically continue $G^A(\xi,\xi';z)$ on the upper half energy plane then $G^A(\xi,\xi';z)$ is no longer bounded when $\xi,\xi'\to\pm\infty$ and it has simple poles at complex values $z=z_n^*$, where an asterisk denotes complex conjugation. As we will later show, the scattering properties of this system are determined by the complex poles of the analytically continued Green's functions. The lifetimes of the quasibound states associated with these complex poles are given by $t_n=1/2|\mathrm{Im}(z_n)|$. Ludviksson [1] has found that the residues of the retarded energy Green's function, at these complex poles, take the form

$$\mathrm{Re\,s}_{z=z_n}G^R(\xi,\xi';z)=\phi_n(\xi)\phi_n(\xi'), \tag{11}$$

where

$$\phi_n(\xi)=\pi\left(-\frac{\partial}{\partial z}G_0^R(0,0;z)\Big|_{z=z_n}\right)^{-1/2}\times\begin{cases} \mathrm{Ci}^{+}(-z_n)\mathrm{Ai}(-\xi-z_n), & \xi\leqslant 0 \\ \mathrm{Ai}(-z_n)\mathrm{Ci}^{+}(-\xi-z_n), & \xi\geqslant 0. \end{cases} \tag{12}$$

The functions $\phi_n(\xi)$ satisfy the Schrödinger equation with complex eigenvalues

$$H(\xi)\phi_n(\xi)=z_n\phi_n(\xi), \tag{13}$$

where z_n are the complex poles of the retarded energy Green's function. The functions $\phi_n(\xi)$ are called generalized eigenstates because they are not square integrable and thus, they do not belong to the Hilbert space. As Nickel and Reichl have shown, the functions $\phi_n(\xi)$ belong to a larger space Φ'_α, where

$$\Phi'_\alpha:=\left\{\phi;\int_{-\infty}^{+\infty}|\phi(\xi)|^2e^{-|\xi|^\alpha}d\xi<\infty\right\} \tag{14}$$

for any $\alpha>\frac{1}{2}$.

It is useful for later reference to introduce the transition spectral density [2], $\rho_E(\xi,\xi')$, defined by

$$\begin{aligned}\rho_E(\xi,\xi')&=\langle\xi|E\rangle\langle E|\xi'\rangle \\ &=\frac{i}{2\pi}\lim_{\delta\to 0}[G^R(\xi,\xi';E+i\delta)-G^A(\xi,\xi';E-i\delta)] \\ &=\frac{i}{2\pi}\sum_n\left[\frac{R^R(\xi,\xi';z_n)}{E-z_n}-\frac{R^A(\xi,\xi';z_n^*)}{E-z_n^*}\right],\end{aligned} \tag{15}$$

where $\langle\xi|E\rangle$ are the continuum eigenstates of the Hamiltonian H, and $R^R(\xi,\xi';z_n)$ are the residues of the Green's function $G^R(\xi,\xi';z)$ evaluated at the poles $z=z_n$, so that

$$R^R(\xi,\xi';z_n)=\mathrm{Re\,s}_{z=z_n}G^R(\xi,\xi';z),$$

and $R^A(\xi,\xi';z_n^*)$ are the residues of the Green's function $G^A(\xi,\xi';z)$ evaluated at the poles $z=z_n^*$, so that

$$R^A(\xi,\xi';z_n^*)=\mathrm{Re\,s}_{z=z_n^*}G^A(\xi,\xi';z),$$

and $R^A(\xi,\xi';z_n^*)=[R^R(\xi,\xi';z_n)]^*$. These quantities will be used when we study light scattering.

III. PARTICLE SCATTERING

In this section, we study the interaction of an incoming particle wave with the potential that consists of a δ-potential well and a static electric field and we compare its reflection with the case when the particle wave interacts only with the static electric field. In this case the δ-potential well acts as a scatterer. We compute the Wigner delay times, which are related with the time that the reflection of the particle wave is delayed due to its interaction with the δ-potential well.

As a first step, let us solve the scattering problem considering only the static electric field. The Schrödinger equation, in dimensionless units, is given by

$$H_0\Psi_E^0(\xi)=\left(-\frac{\partial^2}{\partial\xi^2}-\xi\right)\Psi_E^0(\xi)=E\Psi_E^0(\xi). \tag{16}$$

There are two boundary conditions that have to be satisfied. The first condition is that we can only have a wave incident from the right, since the potential energy given in Eq. (16) becomes infinite as $\xi\rightarrow-\infty$. The second condition is that there is no transmitted wave. The solution that satisfies the above conditions is

$$\Psi_E^0(\xi)=\mathrm{Ci}^-(-\xi-E)-\mathrm{Ci}^+(-\xi-E), \tag{17}$$

where the functions $\mathrm{Ci}^{\pm}(-\xi-E)$ are traveling waves and are defined $\mathrm{Ci}^{\pm}(-\xi-E)=\pm i\mathrm{Ai}(-\xi-E)+\mathrm{Bi}(-\xi-E)$, and E is the energy of the traveling wave. The function Ci^+ represents a wave traveling to the right, while the function Ci^- represents a wave traveling to the left. In Eq. (17), the amplitude of the incident wave Ci^- is normalized to 1. We see that the reflected wave Ci^+ is phase shifted by π, with respect to the incident wave Ci^-.

We now study the scattering of an incident wave for the case when both the δ-potential well and the static electric field are present. In this case, the Schrödinger equation, in dimensionless units, is given by Eq. (4). The scattering solution that satisfies the same two boundary conditions as described above, but which has a discontinuous first derivative at $\xi=0$, is

$$\Psi_E(\xi)=\begin{cases}\mathrm{Ci}^-(-\xi-E)+S(E)\mathrm{Ci}^+(-\xi-E), & \xi\geqslant 0,\\ B(E)\mathrm{Ci}^-(-\xi-E)-B(E)\mathrm{Ci}^+(-\xi-E), & \xi\leqslant 0,\end{cases} \tag{18}$$

where $S(E)$ is the reflection coefficient and is given by

$$S(E)=\frac{\pi V\mathrm{Ai}(-E)^2-i[1-\pi V\mathrm{Ai}(-E)\mathrm{Bi}(-E)]}{\pi V\mathrm{Ai}(-E)^2+i[1-\pi V\mathrm{Ai}(-E)\mathrm{Bi}(-E)]}, \tag{19}$$

and $B(E)$ is the amplitude of the wave for $\xi\leqslant 0$

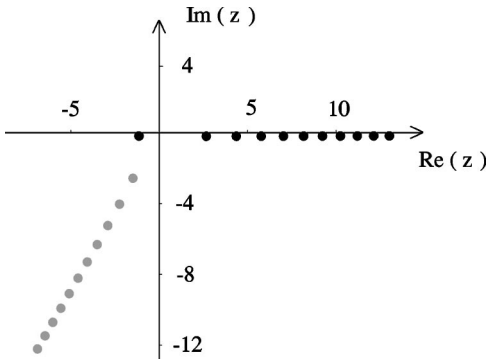

FIG. 1. Dimensionless poles z_n of the retarded energy Green's function G^R in the dimensionless energy range $-7<E<13.5$, for $V=2$. The poles shown as dark circles correspond to the long-lived quasibound states. The long-lived quasibound state with negative energy is a remnant of the bound state in the absence of the static electric field.

$$B(E)=\frac{i}{\pi V\mathrm{Ai}(-E)^2+i[1-\pi V\mathrm{Ai}(-E)\mathrm{Bi}(-E)]}. \tag{20}$$

The reflection coefficient $S(E)$ given in Eq.(19) has absolute value 1, as expected, since there is no transmitted wave. Thus, $S(E)$ can be written as $S(E)=e^{i\theta(E)}$. Comparing Eqs. (19) and (10), we see that when we analytically continue the reflection coefficient $S(E)$ into the lower half complex energy plane it has the same singularities as the retarded energy Green's function G^R. Comparing Eqs. (17) and (18) we see that the effect of the δ-potential well is to cause a phase shift of the reflected wave by $\theta(E)$. The Wigner delay time is the derivative of the phase $\theta(E)$ with respect to the energy

$$\tau_w=\hbar\frac{d\theta(E)}{dE'}=\frac{\hbar}{\epsilon_0}\frac{d\theta(E)}{dE}=\frac{\hbar}{\epsilon_0}\tilde{\tau}_w, \tag{21}$$

where $\tilde{\tau}_w$ is dimensionless. In our case, the Wigner delay time is the time that the reflection of the particle is delayed due to the presence of the δ-potential well. We compute the Wigner delay time for the case that $V=2$. The poles of the retarded energy Green's function for $V=2$ are shown in Fig. 1. For $V=2$, the dimensionless Wigner delay time $\tilde{\tau}_w$ has the form shown in Fig. 2. The phase shift $\theta(E)$ of the incident wave, in the presence of the δ-potential well, is shown in Fig. 3 where $\theta(E)$ is plotted so that it is a continuous function of the energy E.

An interesting feature of the Wigner delay time, shown in Fig. 2, is that it has negative values for certain incident energies and the negative values become larger as the incident energy increases. The negative values indicate that for certain energies the incident particle gets reflected faster when both the static electric field and the δ-potential well are present, as compared to the case when only the static electric field is present. When only the static field is present, a particle with incident energy E reflects at $\xi=-E$. When both

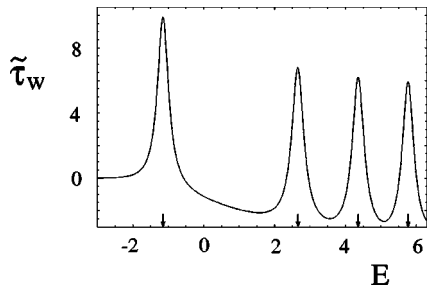

FIG. 2. Dimensionless Wigner delay time $\tilde{\tau}_w$ as a function of the dimensionless incident energy E, for $V=2$. The arrows indicate the energies where the peaks occur.

the static field and the δ-potential well are present, then if the particle's incident energy is negative, $E<0$, the particle first reflects at $\xi=-E>0$, while if the particle's incident energy is positive, $E>0$, the particle first reflects at $\xi=0$. Consequently, for large negative values of the incident energy the particle is not affected by the presence of the δ-potential well, and we find zero Wigner delay times in Fig. 2. However, for increasing positive values of the incident energy the particle begins to be affected by the δ-potential well and can reflect at $\xi=0$, i.e., earlier than it would if no δ-potential well was present.

The Wigner delay time, shown in Fig. 2, has peaks when the energy of the incident particle is very close to the energy of one of the long-lived quasibound states. Actually, the peaks occur at incident energies which are slightly shifted to the left compared to the energies of the long-lived quasibound states (see Table I). These peaks occur because when the incident energy is almost equal to the energy of the long-lived quasibound states, the eigenphase $\theta(E)$ undergoes an abrupt change as can be seen in Fig. 3. In the limit that V becomes very large, the energies of the long-lived quasibound states approach values which are equal to the eigenenergies of a triangular potential well that is formed by the constant electric field and an impenetrable wall located at $\xi=0$ (region I in Fig. 4). Cocke and Reichl [14] have shown for a finite model (a wall is placed far down the hill from the δ-potential well) that the discrete eigenstates with energies very close to the energies of the long-lived quasibound states obtained in Ludviksson's model are very localized. Thus, the long-lived quasibound states correspond to resonance be-

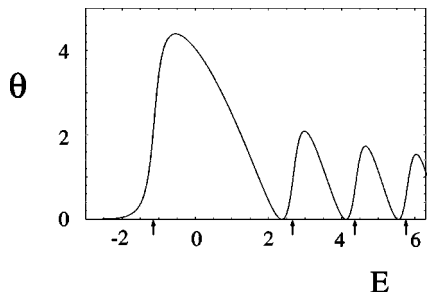

FIG. 3. Phase shift $\theta(E)$ as a function of the dimensionless incident energy E, for $V=2$. The arrows indicate the energies where the peaks in $\tilde{\tau}_w$ occur.

TABLE I. Numerical values for the incident energies E, where the peaks occur in $\tilde{\tau}_w$, as compared to the energies of the long-lived quasibound states z_n, for $V=2$.

E	$\mathrm{Re}(z_n)$
−1.148 59	−1.147 64
2.654 19	2.654 95
4.358 39	4.358 97
5.766 18	5.766 65

tween the potential hill on the left created by the static electric field, and the potential discontinuity created by the δ-potential well.

IV. LIGHT SCATTERING

Let us now study the photodetachment, due to a weak applied time-periodic electric field, of a particle trapped in the δ-potential well. We will compute the single-photon photodetachment rate, assuming dipole coupling between the particle and the time-periodic electric field. We will offer a qualitative comparison of the theoretical results we obtain for the photodetachment rate with the experimental results obtained in the photodetachment of the loosely bound second electron of the H^- ion in the presence of moderate static electric fields [3–5].

A. Theoretical results

The Hamiltonian that describes the interaction of the particle and the time-periodic electric field is given, in terms of dimensionless variables, by

$$H'(\xi)=-\frac{\partial^2}{\partial\xi^2}-\xi-V\delta(\xi)+\mathcal{E}\xi\cos(\omega t), \qquad (22)$$

where $\mathcal{E}$, ω are the strength and the frequency of the time-periodic field using dimensionless variables. $\mathcal{E}=(x_0/\epsilon_0)\mathcal{E}'$, where $\mathcal{E}'$ is the strength of the time-periodic field in units of Joules/m, and $\omega=\omega'\hbar/\epsilon_0$, where ω' is the frequency of the

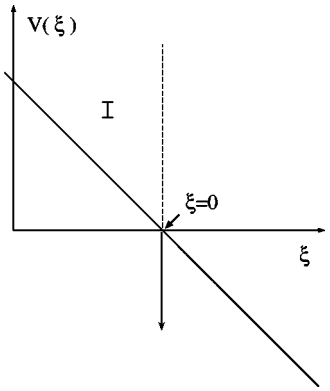

FIG. 4. The dimensionless potential $V(\xi)$ as a function of the dimensionless distance ξ, when both the δ-potential well and the static electric field are present. Region I is the triangular region defined by a vertical line at $\xi=0$ and the static electric field.

time-periodic field in units of rad/sec. Assuming that the time-periodic field is a weak perturbation, we use perturbation theory to find that the photodetachment rate is given by

$$W=\frac{\epsilon_o}{\hbar}2\pi\left(\frac{\mathcal{E}}{2}\right)^2\int_{-\infty}^{+\infty}dE_f|\langle\Psi_{E_f}|\xi|\Psi_0\rangle|^2\delta(E_f-E_0-\omega), \tag{23}$$

where Ψ_0 is the initial state of the particle, and Ψ_{E_f}, defined in Eqs. (6) and (7), are the continuum eigenstates of the Hamiltonian H. We will take as our initial state, $\Psi_0=\sqrt{(V/2)}e^{[-(V/2)|\xi|]}$, which is the bound state of the δ-potential well when no static field is present. The bound state energy, in dimensionless variables, is given by $E_0=-(V/2)^2$. In the presence of the static electric field this state eventually decays. Ludviksson, though, found that the lifetime of this state is given by $V^{-2}e^{V^3/6}$ [1]. Thus, if we consider the attractive δ-potential well to be very deep in comparison with the static electric field, i.e., V is large, the lifetime of the initial state is very large compared to the times of interest here. Therefore, the initial state Ψ_0 when expanded in terms of the energy eigenstates of H is sharply peaked around the energy E_0 and in that sense it is a good approximation to consider the $\delta(E_f-E_0-\omega)$ function in Eq. (23).

We rewrite Eq. (23) as $W=(\epsilon_0/\hbar)\tilde{W}$, where $\tilde{W}$ is dimensionless and is given by

$$\tilde{W}=2\pi\left(\frac{\mathcal{E}}{2}\right)^2\int_{-\infty}^{+\infty}dE_f\int_{-\infty}^{+\infty}d\xi\langle E_f|\xi\rangle\xi\langle\xi|\Psi_0\rangle \times\int_{-\infty}^{+\infty}d\xi'\langle\Psi_0|\xi'\rangle\xi'\langle\xi'|E_f\rangle\delta(E_f-E_0-\omega). \tag{24}$$

In Eq. (24), we used the fact that the continuum eigenstates $\langle\xi|E\rangle$ of the Hamiltonian H are real functions. If we substitute Eq. (15) into Eq. (24), we obtain

$$\begin{aligned}\tilde{W}&=2\pi\left(\frac{\mathcal{E}}{2}\right)^2\int_{-\infty}^{+\infty}d\xi\int_{-\infty}^{+\infty}d\xi'\langle\xi|\Psi_0\rangle\xi\langle\Psi_0|\xi'\rangle\xi'\rho_{E_0+\omega}\times(\xi',\xi)\\&=2\pi\left(\frac{\mathcal{E}}{2}\right)^2\int_{-\infty}^{+\infty}d\xi\int_{-\infty}^{+\infty}d\xi'\langle\xi|\Psi_0\rangle\xi\langle\Psi_0|\xi'\rangle\xi'\times\frac{i}{2\pi}\sum_n\left[\frac{R^R(\xi',\xi;z_n)}{E_0+\omega-z_n}-\frac{R^A(\xi',\xi;z_n^*)}{E_0+\omega-z_n^*}\right]\\&=-\frac{\mathcal{E}^2}{2}\mathrm{Im}\left[\int_{-\infty}^{+\infty}d\xi\int_{-\infty}^{+\infty}d\xi'\langle\xi|\Psi_0\rangle\xi\langle\Psi_0|\xi'\rangle\xi'\times\sum_n\frac{\phi_n(\xi)\phi_n(\xi')}{E_0+\omega-z_n}\right],\end{aligned} \tag{25}$$

where the summation is over the complex poles of the retarded energy Green's function. In Eq. (25), we can interchange the sum and the integral only for a certain class of initial states Ψ_0 for which the integrals

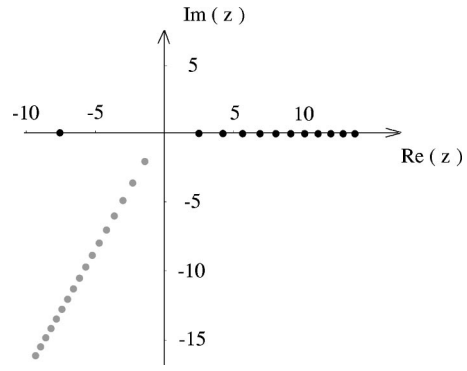

FIG. 5. Dimensionless poles z_n of the retarded energy Green's function G^R in the dimensionless energy range $-9.5<E<14$, for $V=5.5$. The long-lived quasibound state with negative energy is a remnant of the bound state in the absence of the static electric field.

$$\int_{-\infty}^{+\infty}d\xi\langle\xi|\Psi_0\rangle\xi\phi_n(\xi),$$

are well defined. Nickel and Reichl have shown [2] that these initial states must be elements of a space Φ_α where

$$\Phi_\alpha:=\left\{\psi;\int_{-\infty}^{+\infty}|\psi(\xi)|^2e^{|\xi|^\alpha}d\xi<+\infty\right\} \tag{26}$$

for any $\alpha>\frac{1}{2}$. The eigenstate of the δ-potential well, i.e., $\Psi_0=\sqrt{(V/2)}e^{[-(V/2)|\xi|]}$, is an element of the space Φ_α and thus, we safely interchange the sum and the integrals in Eq. (25) to obtain

$$\tilde{W}=-\frac{\mathcal{E}^2}{2}\mathrm{Im}\left[\sum_n\frac{\Gamma_n}{E_0+\omega-z_n}\right], \tag{27}$$

where

$$\Gamma_n=\left(\int_{-\infty}^{+\infty}d\xi\langle\xi|\Psi_0\rangle\xi\phi_n(\xi)\right)^2.$$

We now compute the photodetachment rate for the case $V=5.5$. The reason for the choice of V will become clear when we compare our theoretical predictions with the experimental results for the photodetachment of H^-. In Fig. 5, we show the poles of the retarded energy Green's function for the case $V=5.5$. In Fig. 6 we plot the dimensionless photodetachment rate $\tilde{W}$ as a function of ω, using the com-

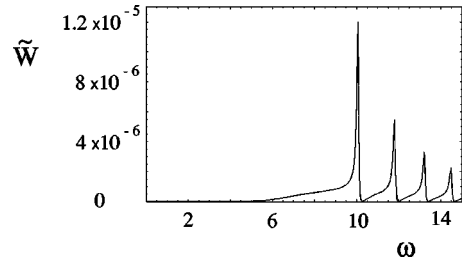

FIG. 6. Dimensionless photodetachment rate $\tilde{W}$ as a function of the dimensionless frequency ω, for $V=5.5$ and $\mathcal{E}=0.01$.

plex poles in the energy range $-10.8<E<27.7$. In all the figures that follow, we take $\mathcal{E}=0.01$. These results are in qualitative agreement with the results of Cocke and Reichl [14] for a finite model and $V=5$.

One of the advantages of using generalized eigenstates to describe the photodetachment rate is that we can directly interpret the main features of the photodetachment rate in terms of the quasibound states of the unperturbed system. In particular, we see from Fig. 6, that the photodetachment rate is strongly enhanced and suppressed for certain frequencies of the weak time-periodic field. The peaks occur when the frequency of the weak time-periodic field is $\omega=E_n-E_0$, where E_0 is the energy of the initial state and $E_n=\mathrm{Re}(z_n)$ are the energies of the long-lived quasibound states z_n with $\mathrm{Re}(z_n)>0$. Thus, the location of the maxima in the photodetachment rate is due to the presence of both the static electric field and the attractive δ-potential well. Also, we see in Fig. 6, that the system makes a transition for frequencies that are below the energy of the bound state, which in our case is given by $E_0=-(V/2)^2$. The lowering of the photodetachment threshold is due to the presence of the static electric field. What is interesting is that the short-lived quasibound states are responsible for the considerable transition rate below the energy $E_0=-(V/2)^2$, as well as for a large amount of the asymmetry that the peaks exhibit in the photodetachment rate $\tilde{W}$, Fig. 6, as we have shown in Ref. [15].

B. Comparison to experimental results

The strong enhancement and suppression of the photodetachment rate for certain frequencies of the weak time-periodic field, that we obtained using the model described by the Hamiltonian H, is also observed experimentally in the photodetachment of H^- ions. [3–5] In these experiments, the photodetachment cross section of the loosely bound second electron of the H^- ion has a ''ripple'' structure, in the presence of moderate static electric fields and using light that is π polarized [3]. (The light is π polarized, when its electric field is parallel to the applied static electric field.)

Theoretical studies on the photodetachment of H^- ion have been carried out by a number of authors [6–10]. These studies use three dimensional models where the final state interaction of the electron with the neutral atom is ignored. They obtain smooth symmetric oscillations in the photodetachment cross section of the H^- ions with the same period as observed experimentally. In what follows, we shall show that our model, which includes final state interaction, also qualitatively reproduces the oscillations observed in the experiments. However, in addition, it predicts strong asymmetries in the oscillations when the static elecric field is large. Since our model is one dimensional our comparison is only qualitative. But, it does suggest that in the three-dimensional models it may be worth including the final state interaction to see if the asymmetries persist.

We first have to relate our parameter V to those used in the experiments, which are the strength of the static electric field and the binding energy, $E_b=0.7542$ eV (where eV denotes electron volts), of the loosely bound second electron. In order to do so, we set

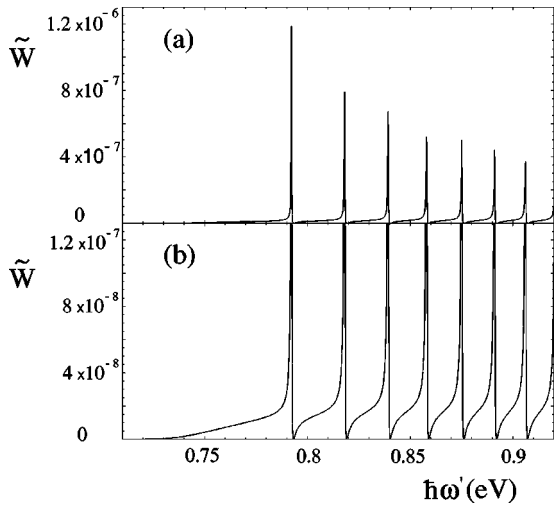

FIG. 7. Dimensionless photodetachment rate $\tilde{W}$ as a function of photon energy $\hbar\omega'$, where the photon energy is expressed in eV, for $\mathcal{E}=0.01$ and $F_1/q=9.2\times10^6$ V/m$\rightarrow V_1=14.3$ and $\epsilon_0=0.0148$ eV. (a) and (b) are the same data but different scales to emphasize different aspects.

$$|E_0'|\equiv\frac{V^2}{4}\epsilon_0=E_b=0.7542\ \text{eV}=1.21\times10^{-19}J. \quad (28)$$

Two values of the static electric field, that were used in the experiments [4] are

$$\frac{F_1}{q}=9.2\times10^6\ \text{V/m}\ \text{ and }\ \frac{F_2}{q}=1.43\times10^7\ \text{V/m}, \quad (29)$$

where $q=1.60\times10^{-19}$ C is the electron charge. These yield $V_1=14.3$ and $V_2=12.3$, respectively, for the strength of the δ-potential well. Thus, the values F_1/q and F_2/q of the static electric field used in the experiment, correspond to very deep δ-potential wells in the model we use.

Using Eq. (24), we now plot, in Figs. 7 and 8, the dimensionless photodetachment rate $\tilde{W}$, for V_1 and V_2, respectively, as a function of photon energy $\hbar\omega'$ expressed in electron volts. Instead of using the complex spectral decomposition, Eq. (27), to compute the photodetachment rate $\tilde{W}$, we have used the continuum eigenstates $\langle E|\xi\rangle$, defined in Eqs. (6) and (7), to obtain $\tilde{W}$ because it is numerically more efficient. Both methods give the same results.

Next, we discuss the features of the experimentally obtained photodetachment cross section of H^- that are qualitatively reproduced by our model. The location of the peaks in the experimentally observed ''ripple'' structure is the same as predicted by our theoretical model. In our model, the maxima in the photodetachment rate occur for frequencies $\omega=E_n-E_0$, in dimensionless units. Thus, using $\epsilon_0\omega=\hbar\omega'$ [see Eq. (2)], we find that the maxima in the photodetachment rate $\tilde{W}$ occur for photon energies, $\hbar\omega'=E_n\epsilon_0+(V/2)^2\epsilon_0$, where E_n are the energies of the long-lived quasibound states with $\mathrm{Re}(z_n)>0$. For large V, the energies E_n are close to the eigenenergies of the triangular well that is formed by the constant electric field and the δ-potential well.

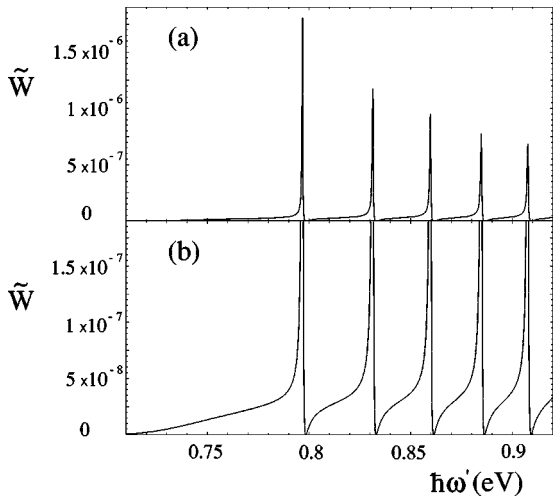

FIG. 8. Dimensionless photodetachment rate $\tilde{W}$ as a function of photon energy $\hbar\omega'$, where the photon energy is expressed in eV, for $\mathcal{E}=0.01$ and $F_2/q=1.43\times10^7$ V/m$\rightarrow V_2=12.3$ and $\epsilon_0=0.0198$ eV. (a) and (b) are the same data but different scales to emphasize different aspects.

Our explanation of the location of the peaks in the photodetachment rate is in agreement with the explanation given by Rau and Wong [7] who used a three dimensional model to explain the experimentally observed photodetachment cross section. In addition, the model we use qualitatively reproduces one more feature that is observed experimentally, that is, the big ''shoulder'' between the energies 0.74 and 0.79 in Fig. 7 and between the energies 0.72 and 0.79 in Fig. 8.

We now focus on the fact that the experimental oscillations appear to be less asymmetric than those we predict theoretically. The asymmetry of the peaks predicted by our model, seen in Figs. 7 and 8, is a result of the presence of both the static electric field as well as the δ-potential well, as we have discussed in Sec. IV A. That is, when the interaction of the final state with the bound state is included it results in asymmetric peaks. Note, that in the three dimensional models [6–10] used to study the photodetachment of H^- where the final state interaction is not included the ''ripple'' structure is smooth and symmetric. One possible explanation for the less asymmetric peaks observed experimentally when compared to those predicted by our model is the following. It would be difficult to observe experimentally the sharp right asymmetric part of the peaks shown in Figs. 7 and 8 due to finite resolution (among other experimental sources of error). It would be of interest to see if for higher values of static electric fields than those used in Refs. [3–5] the experimental results for the photodetachment cross section of the H^- (for π polarized light) would indicate asymmetric peaks, since for higher static electric field values, i.e., smaller V, the theoretical model we use, Fig. 9, predicts asymmetry which extends over a wider range of energies. Therefore, it would be easier to observe experimentally. To illustrate this point, in Fig. 9 we plot the photodetachment rate as a function of the incident photon energy for $V=5.5$. From Eq. (28) we find that when $V=5.5$, the corresponding static electric field is $F/q=1.61\times10^8$ V/m.

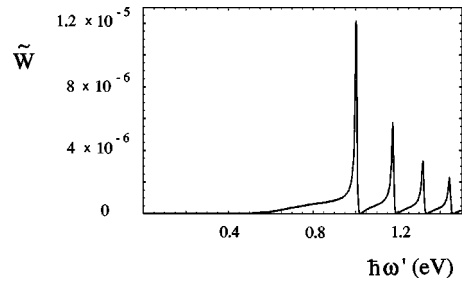

FIG. 9. Dimensionless photodetachment rate $\tilde{W}$ as a function of photon energy $\hbar\omega'$, where the photon energy is expressed in eV, for $\mathcal{E}=0.01$ and $V=5.5\rightarrow F/q=1.61\times10^8$ V/m and $\epsilon_0=0.0997$ eV.

V. CONCLUSIONS

In this paper, we studied the scattering properties of a simple model consisting of single particle states in the presence of a δ-potential well and a static electric field. The importance of this model lies in its simplicity. That is, analytic expressions can be obtained for many of its dynamical properties, such as the scattering properties that we studied in this paper, offering interesting insights into the mechanisms underlying the decay processes of more complex systems. The photodetachment rate computed using the above model, is in qualitative agreement with experimental measurements of the photodetachment cross section of π polarized electromagnetic radiation in H^-.

The asymmetric shape of the photodetachment peaks are a result of the short-lived quasibound state poles, which can be seen in Figs. 1, 5. These asymmetries might be observable experimentally for stronger static electric field strengths than those that have been used up to now. It would be interesting if future experiments could search for those asymmetries.

ACKNOWLEDGMENTS

The authors wish to thank the Robert A. Welch Foundation Grant No. F-1051, NSF Grant No. INT-9602971, the Engineering Research Program of the Office of Basic Energy, and DOE Contract No. DE-FG03-94ER14465 for partial support of this work. The authors also thank Dr. Christoph Jung for useful discussions.

APPENDIX

The simplicity of the model that is described by the Hamiltonian H allows us to easily apply the complex coordinate method [11,12] to this model and discuss some of the main features of this method. The complex coordinate method is a powerful computational technique for the calculation of energies and lifetimes in quantum systems. For systems with a continuum spectrum that are bounded from below, it consists of a complex coordinate rotation, $\xi\rightarrow\xi e^{i\theta}$ whose effect on the spectrum of the transformed Hamiltonian $H(\theta)$ is that the bound states and the branch point where the continuum begins remain invariant while the continuum spectrum ''rotates'' about the branch point by -2θ [11,12]. In the case of the model that is described by the Hamiltonian H, where the continuum spectrum extends from

$-\infty$ to $+\infty$ we apply a complex coordinate translation $\xi \rightarrow \xi + iq$.

Applying the complex coordinate translation, $\xi \rightarrow \xi + iq$, to the energy Green's functions $G^{R/A}(\xi,\xi';z)$, defined in Eqs. (8) and (9), we find that the transformed energy Green's functions $G_q^{R/A}(\xi,\xi';z)$ are given by

$$G_q^{R/A}(\xi,\xi';z) = G_{0,q}^{R/A}(\xi,\xi';z) - \frac{G_{0,q}^{R/A}(\xi,0;z)G_{0,q}^{R/A}(0,\xi';z)}{\frac{1}{V} + G_{0,q}^{R/A}(0,0;z)}, \tag{A1}$$

where $G_{0,q}^{R/A}(\xi,\xi';z)$ are the transformed retarded/advanced energy Green's functions when $V=0$, and are given by

$$G_{0,q}^{R/A} = -\pi \times \begin{cases} \mathrm{Ai}(-\xi - iq - z)\mathrm{Ci}^{\pm}(-\xi' - iq - z), & \xi \leqslant \xi', \\ \mathrm{Ci}^{\pm}(-\xi - iq - z)\mathrm{Ai}(-\xi' - iq - z), & \xi \geqslant \xi'. \end{cases} \tag{A2}$$

In order for $G_q^{R/A}$, $G_{0,q}^{R/A}$ to be bounded when $\xi,\xi' \rightarrow \pm\infty$, z should be given by $z = E - iq \pm i\delta$ for the transformed retarded/advanced energy Green's functions. Thus, the transformed energy Green's functions, $G_q^{R/A}(\xi,\xi';z)$, defined in Eqs. (A1) and (A2), have a cut along the axis $z = E - iq$, while the energy Green's functions $G^{R/A}(\xi,\xi';z)$ have a cut along the real axis. Even though the cut is moved to the lower complex energy plane a distance $-iq$, [11] the complex coordinate translation does not affect the position of the complex poles z_n, which are still defined by Eq. (10).

One of the advantages of the complex coordinate method, is that the residues of the complex poles exposed by the shifted cut, become square integrable functions, as we show in what follows. In particular, in Sec. II we have expressed the residues in terms of the generalized functions $\phi_n(\xi)$, defined in Eq. (12). These are not square integrable functions. From Eqs. (A1) and (A2), we find that the residues of the transformed energy Green's functions are given by

$$\mathrm{Re}\, s_{z=z_n} G_q^R(\xi,\xi';z) = \phi_n^q(\xi)\phi_n^q(\xi'), \tag{A3}$$

where

$$\phi_n^q(\xi) = \pi \left(-\frac{\partial}{\partial z} G_0^R(0,0;z)\Big|_{z=z_n} \right)^{-1/2} \times \begin{cases} \mathrm{Ci}^+(-z_n)\mathrm{Ai}(-\xi - iq - z_n), & \xi \leqslant 0, \\ \mathrm{Ai}(-z_n)\mathrm{Ci}^+(-\xi - iq - z_n), & \xi \geqslant 0. \end{cases} \tag{A4}$$

If we write $z_n = E_n - i\Gamma_n$, then $z_n + iq = E_n + i(q - \Gamma_n) = z_n^q$ and the transformed functions $\phi_n^q(\xi)$ acquire the form

$$\psi_n^q(\xi) = \pi \left(-\frac{\partial}{\partial z} G_1^R(0,0;z)\Big|_{z=z_n} \right)^{-1/2} \times \begin{cases} \mathrm{Ci}^+(-z_n)\mathrm{Ai}(-\xi - z_n^q), & \xi \leqslant 0, \\ \mathrm{Ai}(-z_n)\mathrm{Ci}^+(-\xi - z_n^q), & \xi \geqslant 0. \end{cases} \tag{A5}$$

The transformed functions $\phi_n^q(\xi)$, given in Eq. (A5), are square integrable only when $\mathrm{Im}(z_n^q) > 0$, i.e., $q - \Gamma_n > 0 \Rightarrow 0 < \mathrm{Im}(z_n) < -iq$, which is true for the poles z_n ''exposed'' when the cut shifts by $-iq$. For the poles with $\Gamma_n > q$, the functions $\phi_n^q(\xi)$ are still not square integrable. Thus, in agreement with the complex coordinate method, we find that the eigenfunctions that correspond to the ''exposed'' complex poles are square integrable functions and are given by Eq. (A5), for $0 < \mathrm{Im}(z_n) < -iq$.

In conclusion, the complex coordinate method and the method we have used, both address decaying processes but from a different perspective. In the complex coordinate method the quasibound states are described by square integrable functions that correspond to complex eigenvalues of a non-Hermitian Hamiltonian. In our method the quasibound states are described by generalized eigenstates that are not square integrable (they do not belong to the Hilbert space) that correspond to the complex poles obtained by the analytical continuation of the energy Green's function.

[1] A. Ludviksson, J. Phys. A **20**, 4733 (1987).

[2] J. C. Nickel and L. E. Reichl, Phys. Rev. A **58**, 4210 (1998).

[3] H. C. Bryant, A. Mohagheghi, J. E. Stewart, J. B. Donahue, C. R. Quick, R. A. Reeder, V. Yuan, C. R. Hummer, W. W. Smith, S. Cohen, W. P. Reinhardt, and L. Overman, Phys. Rev. Lett. **58**, 2412 (1987).

[4] J. E. Stewart, H. C. Bryant, P. G. Harris, A. H. Mohagheghi, J. B. Donahue, C. R. Quick, R. A. Reeder, V. Yuan, C. R. Hummer, W. W. Smith, and S. Cohen, Phys. Rev. A **38**, 5628 (1988).

[5] P. G. Harris, H. C. Bryant, A. H. Mohagheghi, C. Tang, J. B. Donahue, C. R. Quick, R. A. Reeder, S. Cohen, W. W. Smith, J. E. Stewart, and C. Johnstone, Phys. Rev. A **41**, 5968 (1990).

[6] I. I. Fabricant, Zh. Eksp. Teor. Fiz. **79**, 2070 (1980).

[7] A. R. P. Rau and H. Wong, Phys. Rev. A **37**, 632 (1988).

[8] W. P. Reinhardt, in *Atomic Excitation and Recombination in External Fields*, edited by M. H. Hayfeh and C. W. Clark (Gordon and Breach, New York, 1985), p. 85.

[9] H. Wong, A. R. P. Rau, and C. H. Greene, Phys. Rev. A **37**, 2393 (1988).

[10] M. L. Du and J. B. Delos, Phys. Rev. A **38**, 5609 (1988).

[11] C. Cerjan, R. Hedges, C. Holt, W. P. Reinhardt, K. Scheibner, and J. J. Wendoloski, Int. J. Quantum Chem. **XIV**, 393 (1978).

[12] W. P. Reinhardt, Annu. Rev. Phys. Chem. **33**, 223 (1982).

[13] *Handbook of Mathematical Functions*, Natl. Bur. Stand. Appl. Math. Ser. No. 55, edited by Abramowitz and I. A. Stegun (U.S. GPO, Washington, DC, 1968).

[14] S. Cocke and L.E. Reichl, Phys. Rev. A **52**, 4515 (1995).

[15] A. Emmanouilidou and L. E. Reichl (unpublished).